Chemical Geology 265 (2009) 420–431

Contents lists available at ScienceDirect

Chemical Geology

journal homepage: www.elsevier.com/locate/chemgeo

The double spike toolbox

John F. Rudge *, Ben C. Reynolds, Bernard Bourdon

Institute of Isotope Geochemistry and Mineral Resources, ETH Zürich, Clausiusstrasse 25, NW, 8092 Zürich, Switzerland

ARTICLE INFO

Article history:
Received 26 February 2009
Received in revised form 1 May 2009
Accepted 10 May 2009

Editor: D. Rickard

Keywords:
Mass spectrometry
Double spike
Optimisation
Fractionation correction

ABSTRACT

The double spike technique is a well established method for correcting for instrumental mass fractionation in mass spectrometry. The precision of the technique is controlled by the choices of double spike composition and the proportions in which the double spike and sample are mixed. To make these choices easier, we provide software ("the double spike toolbox") for calculating optimal double spikes, which are chosen purely on the basis of minimising error propagation. In addition, we provide "cocktail lists" of optimal double spikes for all 33 elements that have 4 or more naturally occurring isotopes, using some sensible default parameters. As examples, we discuss the application of the software to Fe, Pb, and Ca isotopes.

1. Introduction

The double spike technique is a powerful method to correct for instrumental mass fractionation in mass spectrometry. It is an old and well established technique (Dodson, 1963) that is applicable to any element that has four or more isotopes. The double spike technique has received much recent attention due its application in non-traditional stable isotope work (Albarède and Beard, 2004; Fantle and Bullen, 2009), where it is ideally suited to distinguish between natural and instrumental mass fractionation. Double spiking offers a number of advantages over the alternative standard-sample bracketing technique for estimating variations in stable isotope composition: With the double spike, the standard and sample solutions need not be equally pure, and the mass fractionation that occurs during chemical separation can be corrected for. If the double spike equilibrates with the sample prior to chemical separation, quantitative yields and highest purity sample separation are not necessary. However, practical use of the double spike technique may have been slowed by the perceived difficulties of a) obtaining pure spikes, b) determining optimal double spike compositions and double spike-sample mixing proportions, and c) calibrating the double spike.

Key controls on the precision of the double spike technique are the choices of double spike composition and the proportions in which the double spike and sample are mixed. The main aim of this work is to help guide these choices: to make it as easy as possible for experimenters to calculate good double spike compositions whatever isotope system is being studied. To this end, we provide within the electronic appendix MATLAB codes ("the double spike toolbox") that can be used to easily determine optimal double spikes for any isotope system. These codes can be tailored to suit the needs of the individual experimenter. Alongside the codes, we also provide spreadsheets containing lists of optimal double spikes ("cocktail lists") for all 33 elements in the periodic table that have 4 or more naturally occurring isotopes, using some sensible default parameters. Both hypothetical pure spikes and the spikes commercially available from Oak Ridge National Labs, USA have been included in compiling these lists.

The mathematics behind the double spike technique is not new. Indeed, most of the mathematical derivations contained in the appendices here can also be seen in one form or another in the early papers on the subject by Dodson (1963, 1969, 1970) and other authors (Compston and Oversby, 1969; Hofmann, 1971; Russell, 1971; Cumming, 1973; Hamelin et al., 1985). Unfortunately, there have been some slight mistakes made in the more recent literature, particularly regarding error propagation and the determination of optimal double spikes, which we aim to clarify here. A lot of the previous work has focused on particular isotope systems, but the aim here is to be more general and comprehensive.

We begin with a recap of the double spike technique, followed by a discussion of the optimisation. As concrete examples we look at Fe, Pb, and Ca isotopes, and make a comparison with some preliminary experimental data in the case of Fe. Finally, we compare the optimisation approach taken here with that of other authors (Galer, 1999; Johnson and Beard, 1999; Fantle and Bullen, 2009).

2. Overview of the double spike technique

The double spike technique involves measuring the relative amounts of four isotopes, two of which are enhanced by the addition of enriched isotopic spikes to the sample. From knowledge of the double spike

* Corresponding author. Now at: Institute of Theoretical Geophysics, Bullard Laboratories, University of Cambridge, Madingley Road, Cambridge, CB3 0EZ, UK. Tel.: +44 1223 748938; fax: +44 1223 360779.
E-mail addresses: rudge@esc.cam.ac.uk (J.F. Rudge), reynolds@erdw.ethz.ch (B.C. Reynolds), bourdon@erdw.ethz.ch (B. Bourdon).

0009-2541/$ – see front matter © 2009 Elsevier B.V. All rights reserved.
doi:10.1016/j.chemgeo.2009.05.010

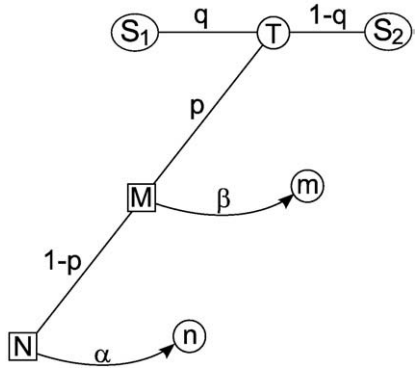

Fig. 1. A schematic diagram of the double spike technique. Lines with arrows represent mass fractionation, lines without arrows represent mixing. The single spikes S_1 and S_2 are mixed in proportions q to $1-q$ (per mole of element) to form the double spike (or tracer) T. N is the natural sample under consideration, which is mixed with the double spike T to form the mixture M. The mixture consists of a proportion p (per mole of element) of double spike to $1-p$ of natural sample. In the mass spectrometer, the mixture M undergoes instrumental mass fractionation with some fractionation factor β so that a different composition m is measured. Similarly, the composition n reflects a mass fractionation from N with a fractionation factor α. For radiogenic isotope work, n is measured in the mass spectrometer from an unspiked run, and so α is another instrumental fractionation factor. For stable isotope work, n is the composition of a standard material, and α reflects the mass fractionation that has occurred in nature. The double spike inversion takes the circled compositions n, m, and T as inputs to determine the unknown α, β, p, N and M.

composition it is possible to invert the measurements to obtain the true composition of the sample corrected for instrumental mass fractionation. A schematic diagram of the technique can be seen in Fig. 1. The double spike (or tracer) T is a mixture of two single spikes S_1 and S_2 (solutions concentrated in a particular isotope). The double spike T is added to a sample N, and the resulting mixture M is measured in a mass spectrometer as m. For isotope systems with a radiogenic isotope, or stable isotope systems which undergo mass-independent natural fractionation, an additional mass spectrometer run is made of the sample alone, known as the unspiked run n. However, the additional run is not necessary for stable isotopes systems which undergo mass-dependent natural fractionation, and n is then the composition of a standard. The mass fractionation that occurs in the mass spectrometer and in nature will be assumed throughout this work to follow a single fractionation law, namely an exponential law, although it should be noted that a lot of the earlier work on the subject has used linear laws (Dodson, 1963, 1969; Hamelin et al., 1985). Different mass fractionation laws are discussed in more detail by Young et al. (2002) and Albarède et al. (2004). Natural variations in stable isotope ratios can be expressed in terms of a mass fractionation factor α from a standard isotope composition n, which can be directly converted to standard δ' notation (Hulston and Thode (1965), Appendix E), e.g. for $^{56}Fe/^{54}Fe$ the exponential fractionation law between sample and standard/unspiked run is

$$\left(\frac{^{56}Fe}{^{54}Fe}\right)_N = \left(\frac{^{56}Fe}{^{54}Fe}\right)_n \left(\frac{55.9349}{53.9396}\right)^{-\alpha}, \quad (1)$$

where 55.9349 and 53.9396 are the atomic weights of ^{56}Fe and ^{54}Fe respectively. Stable isotope variations can be quoted as $\delta'^{56}Fe$, which is linearly related to α by

$$\delta'^{56}Fe = 1000 \log \frac{\left(^{56}Fe/^{54}Fe\right)_N}{\left(^{56}Fe/^{54}Fe\right)_n} = -1000\alpha \log \frac{55.9349}{53.9396}. \quad (2)$$

Similarly, a fractionation factor β describes the mass fractionation occurring in the instrument during measurement of the double spike-sample mixture,

$$\left(\frac{^{56}Fe}{^{54}Fe}\right)_M = \left(\frac{^{56}Fe}{^{54}Fe}\right)_m \left(\frac{55.9349}{53.9396}\right)^{-\beta}. \quad (3)$$

The proportions in which the double spike T and sample N are mixed to form the mixture M can be expressed in terms of a proportion p per mole of element of double spike to $1-p$ of sample, e.g. the mixing law for ^{56}Fe is

$$\left(^{56}Fe\right)_M = p\left(^{56}Fe\right)_T + (1-p)\left(^{56}Fe\right)_N, \quad (4)$$

where (^{56}Fe) denotes the molar proportion of Fe that is ^{56}Fe. The mass fractionation laws (1) and (3) and the mixing law (4) form the governing equations for the double spike technique.

Given the double spike composition T, measurements of the mixture m, and measurements of the unspiked run/standard composition n, it is possible to invert to find the true composition of the sample N, the mixture M, double spike to sample proportion p, and the fractionation factors α and β. The relative amounts of the four isotopes can be expressed in terms of three isotopic ratios with common denominator e.g. $^{56}Fe/^{54}Fe$, $^{57}Fe/^{54}Fe$, $^{58}Fe/^{54}Fe$. The inversion involves the solution of three simultaneous non-linear equations (one for each isotopic ratio) for the three unknowns p, α, and β. This can be done iteratively, and the procedure is described in detail in Appendix A. It should be particularly noted that the results of the inversion depend only on the relative amounts of the four isotopes, and not on how these relative amounts are expressed in the calculations: In particular, the results of the inversion are independent of the choice of denominator isotope (Mel'nikov, 2005).

3. Optimising the double spike

To judge a double spike to be optimal an objective criterion is needed that determines how good a particular double spike is. A very natural criterion for a good double spike is one which produces low errors (Cumming, 1973). Indeed, the whole aim of double spiking is to get precise measurements: the more precise the better. However, there is still the question of which error to minimise. For stable isotope work, it seems natural to minimise the error on the fractionation factor α between standard and sample since it is the mass fractionation processes that occur in nature that are of interest. For radiogenic isotope work, we may be interested instead in a particular isotopic ratio, and it is the error on that particular ratio which we wish to minimise. These different choices of which error to minimise will lead to slightly different optimal double spikes, as we shall discuss later in the context of Pb isotopes.

To calculate the errors for a particular double spike we must first specify a model of the errors in the inputs n, m, and T (Appendix C). By default, the error model used in the software assesses the expected internal precision of the technique rather than its accuracy. For the mixture measurements m, the default error model is that of independent ion beams whose intensities are measured with errors due to a) Johnson–Nyquist noise of the impedance amplifiers (thermal noise of the electronic baseline) and b) counting statistics of the ion beam intensities (shot noise). It is assumed that the mean total ion beam intensity of the element remains constant (10 V by default [100 pA on 10^{11} Ω resistors], but adjustable). The double spike composition T is assumed to have no error, since its composition is fixed and does not fluctuate during the course of a mass spectrometer run. Similarly, for stable isotope work it is also assumed that the standard composition n has no error, but for radiogenic isotope work it is assumed that the unspiked run n has instrumental errors similar to m.

The default error model represents a best case scenario, and applies to any isotope system and mass spectrometer. In practice, there may be additional sources of error that depend on the details of the particular isotope system and mass spectrometer and these must be dealt with on a case by case basis e.g. additional errors can arise due to corrections for interferences, acid blanks, and hydride/oxide production. The software allows for customisation of the error model

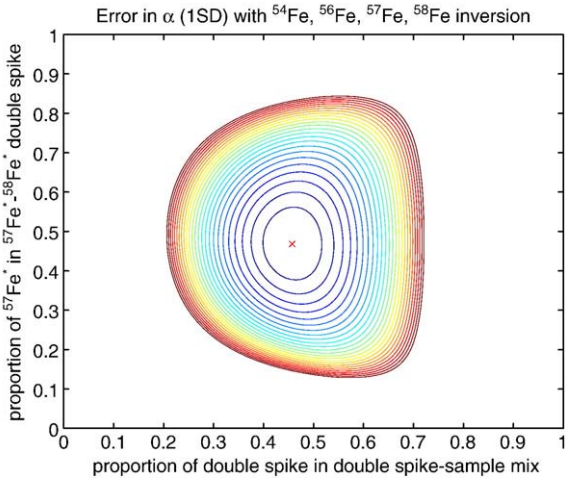

Fig. 2. Contour plot of error in α for the ^{57}Fe*–^{58}Fe* ORNL double spike. The horizontal axis gives the proportion p of double spike in the double spike-sample mixture, and the vertical axis gives the proportion q of ^{57}Fe* in the double spike. The optimum is marked by a cross, with 45.74% double spike to 54.26% sample with a double spike of 46.80% ^{57}Fe* to 53.20% ^{58}Fe* (see Table 2). The plot is thresholded so that only contours within 25% of the optimal error are shown, and contours are evenly spaced with interval 1% of the optimal error on α. Note that there is quite a broad region around the optimum where low errors are found.

(see Appendix C), and can be used to explore some of these additional sources of error. All the calculations shown here use the default error model.

While the double spike and standard compositions do not fluctuate, the compositions themselves may not be known accurately, and this can lead to systematic biases (inaccuracies) in the results of the double spike inversion. These biases can be reduced by good calibration, and calibration is discussed further in Appendix F. Since we are only usually interested in the composition of the sample *relative* to the standard, it is not necessary to know accurately the absolute composition of the standard, but only the mass fractionation line on which it lies. Similarly, it is not necessary to know the absolute composition of the double spike, only its composition relative to the chosen standard value.

Once an error model has been specified, the errors have to be propagated through the double spike inversion procedure to get the errors on the quantities of interest, such as α. There are two main approaches to error propagation: Monte Carlo simulation and linear error propagation. Monte Carlo simulations are by far the easiest to code, but are slower and give answers that vary slightly each time the code is run. Linear error propagation is more involved to code as it requires calculating various partial derivatives and performing matrix manipulations (Appendix B), but once coded it is much faster and there is no variability in the answer. Linear error propagation is only valid for small errors, but this holds true here. For optimisation of the double spike, linear error propagation is much preferred for its speed and the fact that the estimated error varies smoothly with changes in parameters. However, Monte Carlo simulations are still useful to verify that the linear error propagation is accurate, and a routine for performing Monte Carlo simulations is available in the software.

We calculate the expected errors using linear error propagation. The errors are given as the theoretical standard deviation for repeated measurements (each measurement is an 8-second integration by default). Given 100 repeated measurements the analytical precision should thus be 5 times smaller than this if given as 2 standard errors of the mean. If the errors are doubled, 4 times as many repeat measurements are required to obtain the same internal analytical precision. Note that typically thermal noise is much less than shot noise (thermal noise has a standard deviation of 0.01 mV by default), and so the default errors scale approximately with the square root of mean total beam intensity provided this intensity is not too low.

Given the 4 isotopes used in the inversion, there are 6 possible double spikes. Once one of these possibilities is chosen, there are then two parameters we can vary: the proportion q (by mole of element) in which the two single spikes are mixed to form the double spike, and the proportion p in which the double spike is mixed with the sample (Fig. 1). q describes a mixing law similar to that for p in Eq. (4), e.g.

$$\left(^{56}\mathrm{Fe}\right)_T = q\left(^{56}\mathrm{Fe}\right)_{S_1} + (1-q)\left(^{56}\mathrm{Fe}\right)_{S_2}. \quad (5)$$

The single spikes S_1 and S_2 may be hypothetical pure spikes, or real spikes which contain small amounts of the other isotopes, such as those commercially available from Oak Ridge National Labs (ORNL). The optimisation works identically in both cases. We will denote the ORNL spikes by an asterisk (*) to distinguish them from the hypothetical pure spikes.

An example of this is shown in Fig. 2, where a contour plot of the error in α is shown for a ^{57}Fe*–^{58}Fe* ORNL double spike as a function of p and q. The error surface is bowl-shaped with a single minimum. Finding the optimal double spike is simply a matter of locating this minimum, which is done effectively with gradient methods (Appendix D). The contour plot is useful not only because it shows the optimal double spike, but also because it gives an idea of how robust the optimal double spike is: Often we cannot mix in exactly the proportions we would like as the sample concentration is not well known, and so it is important to understand how the error varies in the vicinity of the optimum. In the particular example of Fig. 2, the optimum is quite robust as the error surface is very flat there. Indeed, for this example there are a wide range of values of p and q that are within 25% of the optimum error on α. It should be noted that the optimal values of p and q depend only slightly on the actual sample composition and mass fractionation factors. Thus once the optimal double spike composition and double spike-sample mixing proportions have been determined for a standard composition, they can then be used effectively for measurement of all samples.

4. Examples

4.1. Fe

As a concrete example, we now consider Fe in more detail, which has four naturally occurring isotopes: ^{54}Fe, ^{56}Fe, ^{57}Fe, and ^{58}Fe. The 6 possible double spikes are ^{54}Fe–^{56}Fe, ^{54}Fe–^{57}Fe, ^{54}Fe–^{58}Fe, ^{56}Fe–^{57}Fe, ^{56}Fe–^{58}Fe, and ^{57}Fe–^{58}Fe. The results of optimising the error on α for each of these pairs for pure spikes are shown in Table 1. The different choices of double spike have been ranked in order of increasing error. A ^{56}Fe–^{58}Fe double spike appears to be best, with an optimal composition of 77.28% ^{56}Fe to 22.72% ^{58}Fe and 55.40% double spike to 44.60% sample. The ^{57}Fe–^{58}Fe double spike is a close second.

Lower down the table in fourth place is the ^{54}Fe–^{58}Fe double spike, which has been used by a number of researchers (Johnson and Beard,

Table 1
Optimal double spikes for Fe isotopes using pure spikes.

Double spike composition				Mixture composition		Error estimates (1SD)	
^{54}Fe	^{56}Fe	^{57}Fe	^{58}Fe	Double spike	Sample	Error in α	ppm/amu
	77.28%		22.72%	55.40%	44.60%	0.0032	57
		47.65%	52.35%	44.86%	55.14%	0.0035	62
	75.31%	24.69%		69.16%	30.84%	0.0045	80
79.96%			20.04%	21.48%	78.52%	0.0093	166
44.87%	55.13%			39.82%	60.18%	0.0109	193
70.23%		29.77%		23.06%	76.94%	0.0263	469

All 6 possible double spikes have been considered. Errors are for a 10 V mean total beam intensity with 8-second integrations. The ppm/amu column gives a rescaling of the error in α to give an approximate estimate of parts per million per atomic mass unit errors on the isotope ratios (the scaling factor is 10^6/mean atomic mass, see Appendix E). The ^{56}Fe–^{58}Fe double spike has the lowest error, closely followed by the ^{57}Fe–^{58}Fe double spike. The Fe standard composition is (5.85%, 91.75%, 2.12%, 0.28%) (Rosman and Taylor, 1998).

Table 2
Optimal double spikes for Fe using the spikes available from Oak Ridge National Labs (ORNL).

Double spike composition				ORNL proportions				Mixture composition		Error estimates (1SD)	
^{54}Fe	^{56}Fe	^{57}Fe	^{58}Fe	^{54}Fe*	^{56}Fe*	^{57}Fe*	^{58}Fe*	Double spike	Sample	Error in α	ppm/amu
0.15%	79.57%	0.33%	19.96%		76.41%		23.59%	55.86%	44.14%	0.0033	59
0.25%	10.59%	44.13%	45.02%			46.8%	53.2%	45.74%	54.26%	0.0036	65
0.08%	76.54%	23.37%	0.02%		74.87%	25.13%		69.61%	30.39%	0.0046	83
78.63%	4.01%	0.31%	17.04%	79.86%			20.14%	21.21%	78.79%	0.0095	169
42.93%	57.01%	0.05%	0.01%	43.6%	56.4%			40.14%	59.86%	0.0111	197
69.06%	3.17%	27.75%	0.02%	70.17%		29.83%		23.28%	76.72%	0.0267	476

The ORNL spike compositions are ^{54}Fe* = (98.37%, 1.55%, 0.07%, 0.01%), ^{56}Fe* = (0.07%, 99.88%, 0.04%, 0.01%), ^{57}Fe* = (0.10%, 6.97%, 92.88%, 0.05%), and ^{58}Fe* = (0.39%, 13.78%, 1.25%, 84.58%). Errors are again for a 10 V mean total beam intensity with 8-second integrations. The errors are only slightly worse than for the pure spikes shown in Table 1.

1999). The proportions found optimal by Johnson and Beard (1999) have ~90% ^{54}Fe to ~10% ^{58}Fe, which is not too dissimilar to the 79.96% ^{54}Fe to 20.04% ^{58}Fe given in Table 1. However, the calculations suggest that three times greater precision could be gained by moving to either the ^{56}Fe–^{58}Fe or ^{57}Fe–^{58}Fe double spikes, which have been used in more recent work (Konter et al., 2008b,a; Lacan et al., 2008).

As remarked earlier, the commercially available spikes contain impurities, and the corresponding optimal double spikes for the Fe spikes sold by ORNL are shown in Table 2. Note that this table has extra columns, distinguishing the proportions in which the impure ORNL spikes are mixed from the actual isotopic proportions in the double spike. Spike purity has only a small impact here: the optimal ORNL ^{57}Fe*–^{58}Fe* double spike contains 10.84% impurities as ^{54}Fe and ^{56}Fe, and yet the error on α is only 4% worse than for the pure ^{57}Fe–^{58}Fe double spike. It has been found that in many isotope systems spike purity has only a negligible effect (Russell, 1971), but it is easy to explore the effects of spike purity in detail with the software we provide.

A useful plot for comparing the different double spikes is shown in Fig. 3, where the error in each of the optimal double spikes given in Table 2 is shown as a function of the proportion p of double spike in the mixture. The fact that these curves are fairly flat around the minimum for the ^{56}Fe*–^{58}Fe* and ^{57}Fe*–^{58}Fe* double spikes demonstrates their robustness to changes in the double spike-sample mix. Indeed the fact that the ^{57}Fe*–^{58}Fe*curve is flatter than the ^{56}Fe*–^{58}Fe* curve may be one reason to prefer the ^{57}Fe*–^{58}Fe* double spike despite its slightly greater error.

The theoretical error estimates can be tested experimentally, and an example of this is shown in Fig. 4. A double spike consisting of 50% ^{57}Fe* and 50% ^{58}Fe* (ORNL) was added to a standard in a range of different proportions. The resulting mixtures were measured by MC-ICP-MS, and the within run error on α calculated (for further experimental details, see Appendix G). These preliminary experimental results lie fairly close to the theoretical curves, providing some good validation for the theory. For this particular example the default error model successfully accounts for most of the error that is observed, but in other situations there may well be additional sources of error (e.g. from interference corrections) that are not accounted for in the default error model. Work on the practical development of the Fe double spike using MC-ICP-MS is ongoing, and is a topic for a future manuscript. For practical details on the implementation of Fe isotope mass spectrometry the reader is referred to the literature (Johnson and Beard, 1999; Kehm et al., 2003; Fantle and Bullen, 2009).

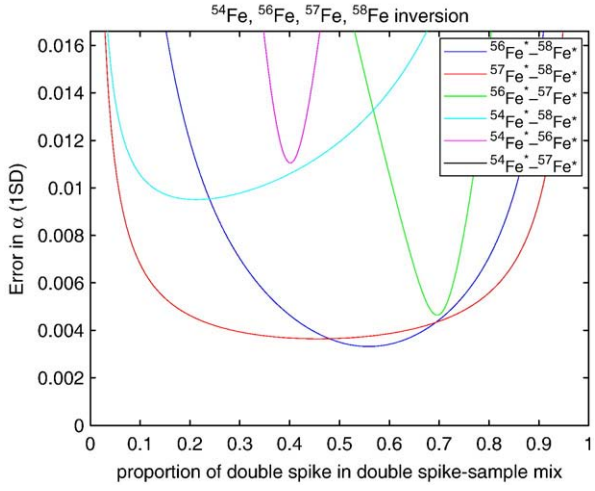

Fig. 3. Plot of error in α against proportion p of double spike in double spike-sample mixture for the optimal ORNL Fe double spikes (compositions given in Table 2). The ^{54}Fe*–^{57}Fe* double spike is outside the plot range. The ^{57}Fe*–^{58}Fe* curve here is a 1D transect of the contour plot in Fig. 2 at the optimal double spike composition of 46.80% ^{57}Fe* to 53.20% ^{58}Fe*.

4.2. Pb

The Pb double spike has been much studied (Dodson, 1969; Compston and Oversby, 1969; Dallwitz, 1970; Hofmann, 1971; Cumming, 1973; Hamelin et al., 1985; Galer, 1999; Mel'nikov, 2005). Like Fe, there are just four naturally occurring isotopes of Pb: ^{204}Pb, ^{206}Pb, ^{207}Pb, ^{208}Pb; but unlike Fe, Pb is a radiogenic system. As such, n now represents an additional mass spectrometer run (the unspiked run), and α is the instrumental fractionation associated with this run. In choosing the optimal double spike for radiogenic systems it is more natural to minimise the

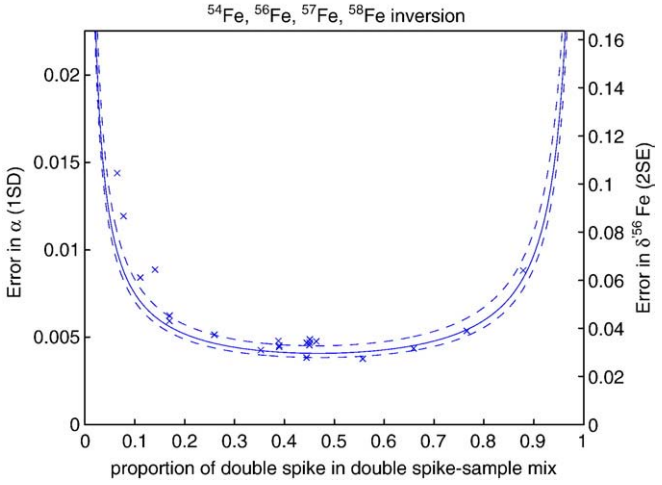

Fig. 4. Comparison of theoretical curves with MC-ICP-MS data for Fe. The double spike consists of 50% ^{57}Fe* and 50% ^{58}Fe*, near the calculated optimum composition. The solid line is a theoretical curve for a total mean beam intensity of 15.3 V with four-second integrations. In the experiments the total beam intensity was not precisely controlled, but varied from 12.7 to 17.1 V over the different runs, and the theoretical curves for these intensities are shown as dashed lines. Each data point on the plot (crosses) is based on experimental results from 100 four-second integrations. The general agreement between theory and experiment is encouraging, although the match is not perfect. The right hand side y-axis re-expresses the standard deviation on α as the 2 standard error on δ'^{56}Fe, which is more typically reported (the scaling factor is $1000\log(55.9349/53.9396)\times 2/\sqrt{100}$, Appendix E).

Table 3
Optimal double spikes for Pb isotopes using pure spikes.

Double spike composition				Mixture composition		Error estimate (1SD)
^{204}Pb	^{206}Pb	^{207}Pb	^{208}Pb	Double spike	Sample	Error in ^{206}Pb/^{204}Pb
63.44%		36.56%		51.24%	48.76%	0.0031
72.90%	27.10%			50.73%	49.27%	0.0032
	71.83%	28.17%		52.74%	47.26%	0.0034
22.19%			77.81%	56.29%	43.71%	0.0045
		10.93%	89.07%	61.50%	38.50%	0.0048
	37.68%		62.32%	53.37%	46.63%	0.0056
Double spike composition				Mixture composition		Error estimate (1SD)
^{204}Pb	^{206}Pb	^{207}Pb	^{208}Pb	Double spike	Sample	Error in ^{207}Pb/^{204}Pb
53.85%		46.15%		52.92%	47.08%	0.0031
72.97%	27.03%			47.01%	52.99%	0.0032
	76.04%	23.96%		56.48%	43.52%	0.0044
21.50%			78.50%	54.49%	45.51%	0.0052
		10.10%	89.90%	62.70%	37.30%	0.0060
	38.60%		61.40%	54.91%	45.09%	0.0077
Double spike composition				Mixture composition		Error estimate (1SD)
^{204}Pb	^{206}Pb	^{207}Pb	^{208}Pb	Double spike	Sample	Error in ^{208}Pb/^{204}Pb
56.63%		43.37%		48.94%	51.06%	0.0079
69.94%	30.06%			46.74%	53.26%	0.0083
	78.04%	21.96%		56.77%	43.23%	0.0131
20.62%			79.38%	55.16%	44.84%	0.0159
		9.62%	90.38%	64.11%	35.89%	0.0192
	38.27%		61.73%	55.79%	44.21%	0.0250

Errors are for a 10 V mean total beam intensity with 8-second integrations for both the spiked and unspiked runs. The optimal double spikes in these three tables minimise the error in the sample ^{206}Pb/^{204}Pb, ^{207}Pb/^{204}Pb, and ^{208}Pb/^{204}Pb ratios respectively. In all cases, the ^{204}Pb–^{207}Pb double spike has the lowest error, although the optimal proportions vary slightly. The Pb standard composition is (1.40%, 24.10%, 22.10%, 52.40%) (Rosman and Taylor, 1998).

error on a particular isotopic ratio rather than α (Cumming, 1973). Which ratio to choose depends on the particular application.

An example is shown in Table 3, where optimal pure double spikes are shown which minimise the error on three different isotopic ratios: ^{206}Pb/^{204}Pb, ^{207}Pb/^{204}Pb, and ^{208}Pb/^{204}Pb. In each case, the much used ^{204}Pb–^{207}Pb double spike is optimal, with the ^{204}Pb–^{206}Pb double spike a close second. The optimal proportions vary slightly with the different choices of ratio, but all have fairly equal amounts of ^{204}Pb to ^{207}Pb. Minimising the error on α gives a fairly similar result, with 49.12% ^{204}Pb to 50.88% ^{207}Pb. These optimal proportions are not too dissimilar to those originally proposed by Dodson (1969) and Cumming (1973) (~33% ^{204}Pb to ~67% ^{207}Pb), although all have slightly more ^{204}Pb. If instead the error on the sample ^{207}Pb/^{206}Pb ratio is minimised, the optimal double spike is much closer to that proposed by Dodson (1969) and Cumming (1973), with 35.24% ^{204}Pb to 64.76% ^{207}Pb.

4.3. Ca

Ca is a stable isotope system with six naturally occurring isotopes: ^{40}Ca, ^{42}Ca, ^{43}Ca, ^{44}Ca, ^{46}Ca, ^{48}Ca. For elements with more than four isotopes an additional choice must be made: which four isotopes to use in the inversion. An example is shown in Table 4, where the optimal double spikes for all possible choices of the four isotopes have been calculated. In this case, the optimal choice of isotopes for the inversion is ^{40}Ca, ^{42}Ca, ^{44}Ca, and ^{48}Ca using a ^{42}Ca–^{48}Ca double spike. The error surface for this double spike is shown in Fig. 5. In fact, this double spike is exactly what was used in the pioneering work on Ca isotopes by Russell et al. (Russell et al., 1978; Russell and Papanastassiou, 1978), although the proportions chosen were somewhat different. More recent work has used double spike compositions with roughly equal

Table 4
Optimal double spikes for Ca isotopes using pure spikes.

Double spike composition						Mixture composition		Error estimates (1SD)	
^{40}Ca	^{42}Ca	^{43}Ca	^{44}Ca	^{46}Ca	^{48}Ca	Double spike	Sample	Error in α	ppm/amu
	39.64%				60.36%	14.24%	85.76%	0.0015	35
	46.42%			53.58%		17.53%	82.47%	0.0016	37
		43.53%			56.47%	16.96%	83.04%	0.0016	37
		48.98%		51.02%		22.39%	77.61%	0.0018	40
			16.05%		83.95%	12.74%	87.26%	0.0019	43
			15.5%		84.5%	12.57%	87.43%	0.0019	44
			15.45%		84.55%	12.52%	87.48%	0.0019	44
				47.25%	52.75%	31.49%	68.51%	0.0021	48
			22.98%	77.02%		17.80%	82.20%	0.0023	52
			22.38%	77.62%		17.62%	82.38%	0.0023	53
			21.62%	78.38%		17.25%	82.75%	0.0024	54
	48.27%	51.73%				42.46%	57.54%	0.0026	60
	21.26%			78.74%		4.68%	95.32%	0.0042	96
		37.66%		62.34%		6.38%	93.62%	0.0050	115
	29.33%	70.67%				15.51%	84.49%	0.0057	129
	7.41%		92.59%			19.54%	80.46%	0.0059	135
		30.98%		69.02%		5.17%	94.83%	0.0061	140
			44.62%	55.38%		8.81%	91.19%	0.0062	141
	12.21%			87.79%		3.16%	96.84%	0.0063	143
		11.9%			88.1%	6.85%	93.15%	0.0063	143
	4.29%				95.71%	5.70%	94.30%	0.0064	146
	3.75%			96.25%		5.70%	94.30%	0.0068	155
		47.74%		52.26%		5.58%	94.42%	0.0072	165
		53.63%		46.37%		6.55%	93.45%	0.0073	167
				30.84%	69.16%	13.67%	86.33%	0.0073	168
		34.93%			65.07%	6.96%	93.04%	0.0074	169
			15.84%		84.16%	6.20%	93.80%	0.0074	169
			16.05%		83.95%	6.19%	93.81%	0.0074	170
			32.11%	67.89%		6.28%	93.72%	0.0075	171
				35.14%	64.86%	11.49%	88.51%	0.0080	182
		17.25%	82.75%			27.73%	72.27%	0.0082	188

Errors are for a 10 V mean total beam intensity with 8-second integrations. Columns are the same as in Table 1 with additional highlighting showing the choice of 4 isotopes used in the inversion. Ca has 6 naturally occurring isotopes, and thus 15 possible choices of the 4 isotopes to use in the inversion and a total of 90 possible double spikes. Only those with errors less than 200 ppm/amu are shown here (the full list can be found in the cocktail list in the electronic appendix). The Ca standard composition is (96.94%, 0.65%, 0.14%, 2.09%, 0.00%, 0.19%) (Rosman and Taylor, 1998).

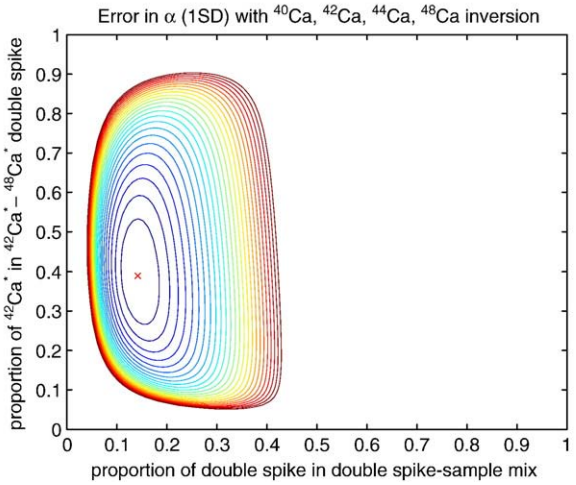

Fig. 5. Contour plot of error in α for the ^{42}Ca*–^{48}Ca* ORNL double spike using ^{40}Ca, ^{42}Ca, ^{44}Ca, and ^{48}Ca in the inversion. The horizontal axis gives the proportion p of double spike in the double spike-sample mixture, and the vertical axis gives the proportion q of ^{42}Ca* in the double spike. The optimum is marked by a cross, with 14.17% double spike to 85.83% sample with a double spike of 38.92% ^{42}Ca* to 61.08% ^{48}Ca*. The plot is thresholded so that only contours within 25% of the optimal error are shown, and contours are evenly spaced with interval 1% of the optimal error on α. Again there is quite a broad region around the optimum where low errors are found. The ORNL spike compositions are ^{42}Ca* = (4.88%, 94.48%, 0.07%, 0.55%, 0.01%, 0.01%) and ^{48}Ca* = (2.10%, 0.02%, 0.01%, 0.07%, 0.01%, 97.78%).

amounts of ^{42}Ca to ^{48}Ca, very close to the optimum calculated here (see review by DePaolo, 2004 for more details). The use of ^{40}Ca as an inversion isotope is sometimes problematic because of the existence of radiogenic anomalies from the decay of ^{40}K, but in many stable isotope studies (e.g. carbonate systems) such radiogenic anomalies are negligible. For cosmochemistry applications there may also be variations in the amount of natural ^{48}Ca due to s-process nuclides.

Since the error estimates are based on comparing the same total amount of Ca ions, but only some of the ions are used in the inversion, there is a bias towards using the more abundant natural isotopes in the inversion. In Table 4, over 97% of the total Ca ions are used in the inversions which include ^{40}Ca (the most abundant natural isotope), but less than 14% of the Ca ions are used in the inversions without ^{40}Ca. When the total beam intensities are scaled so that the sum of the ion beams used in the inversion is kept constant instead, the lowest error estimates are for inversions without ^{40}Ca. In fact, the lowest error is for a ^{43}Ca–^{46}Ca double spike, using ^{42}Ca, ^{43}Ca, ^{46}Ca, and ^{48}Ca in the inversion. This is important for the applicability of double spike techniques to the measurement of Ca stable isotope variations by MC-ICP-MS, where the ^{40}Ca ion beam cannot be accurately measured due to the interference of ^{40}Ar.

Unlike Fe and Pb, spike purity has a noticeable effect for Ca, particularly for those double spikes which use a ^{46}Ca spike. The ORNL ^{46}Ca* spike is notably impure, with less than a third of the total Ca isotopes in the spike being ^{46}Ca. The effect this impurity has on the error on α is shown in Fig. 6 for the ^{42}Ca–^{46}Ca double spikes. While the ^{42}Ca–^{46}Ca double spike ranks second amongst the pure double spikes (Table 4), the ^{42}Ca*–^{46}Ca* ranks only sixth amongst the ORNL double spikes (electronic appendix). As a result of the impurity, the error on α increases by 28%.

There has been considerable discussion in the literature about which double spikes provide the lowest errors for Ca (Gopalan et al., 2006, 2007; Fantle and Bullen, 2009; Feineman et al., 2009). However, the choice of double spike is but one factor of many that go into generating precise and accurate measurements. In particular, since internal precisions are typically much better than external reproducibility for Ca, errors are not ultimately limited by the chosen double spike composition, but by the instrumentation (Fantle and Bullen, 2009). Potentially this problem could be minimised in several ways that are dependent upon the source of the additional error: for example, by choosing inversion isotopes of limited dynamic range to minimise ion-optic effects within the mass spectrometer (e.g. a ^{42}Ca–^{43}Ca double spike with a ^{40}Ca, ^{42}Ca, ^{43}Ca, ^{44}Ca inversion, Holmden, 2005), or by neglecting ^{40}Ca which requires a large dynamic range of measured currents if non-linearity in amplifier response is problematic.

5. Double spike cocktail lists

The methods that have been described above can be applied to any of the 33 elements that have four or more naturally occurring isotopes. For each element we have produced tables of optimum double spikes that minimise the error on α (as in Tables 1, 2, and 4). These are available as two spreadsheets in the electronic supplement. One spreadsheet provides the optimal pure double spikes, and the other provides the optimal ORNL double spikes.

The recipes in these "cocktail lists" should prove very useful in choosing good double spikes, but as with all good recipes they should be taken with a pinch of salt: As has been pointed out in the examples, there are a number of other factors that are important in choosing a good double spike that have not been taken into account in producing the cocktail lists. For example, if it is difficult to mix in the desired proportions, then the flatness of the error surface near the optimum is important. Often there are interferences on certain isotopes, or the mass spectrometer may only be able to measure a particular mass range, excluding some isotopes from consideration. The cocktail list double spike compositions minimise the error on α rather than on particular isotopic ratios, and so may not be as well suited to radiogenic systems. Problems such as these need to be dealt with on a case by case basis, and the "double spike toolbox" software is provided to help with this.

It should be noted that the whole double spike technique is reliant on the chosen mass fractionation law being an accurate description of the processes occurring in nature and in the mass spectrometer — if this is not so (Vance and Thirlwall, 2002; Thirlwall, 2002; Thirlwall and Anczkiewicz, 2004), e.g. due to mass-independent fractionations, or due to different mass-dependent fractionations occurring than expected, then the whole method breaks down. Large interferences are also particularly troublesome for the double spike technique if they cannot be corrected for, and can cause spurious results to be

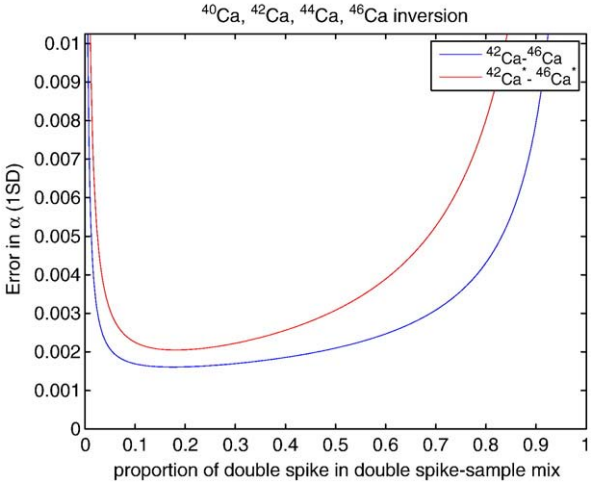

Fig. 6. An example of the effect of spike purity. Shown is the error in α for the optimal pure ^{42}Ca–^{46}Ca double spike (46.42% to 53.58%) and the optimal ORNL ^{42}Ca*–^{46}Ca* double spike (32.99% to 67.01%) as a function of the proportion of double spike in the double spike-sample mix. ^{40}Ca, ^{42}Ca, ^{44}Ca, and ^{46}Ca are used in the inversion. The ORNL ^{46}Ca* spike is not very pure, and is less than a third ^{46}Ca: the composition is ^{46}Ca* = (60.79%, 0.76%, 0.19%, 5.69%, 30.91%, 1.65%). The impurity leads to a 28% larger error at the optimum.

produced on inversion. It should also be reiterated that the accuracy of the technique is dependent on good calibration of the double spike, without which systematic biases can occur (Appendix F).

6. Alternative approaches

The methodology of this work is largely based on the algebraic approach of Dodson (1969), Cumming (1973), and Hamelin et al. (1985). Alternative geometrical methods for double spike optimisation have been proposed by Galer (1999, 2007, 2008) and Johnson and Beard (1999). One geometrical idea proposed by these authors is that an optimal double spike should maximise the angle θ between the planes defined by $N-n-T$ and $M-m-T$ in a particular isotope ratio space (Hofmann, 1971; Russell, 1971). While it is certainly true that double spikes with angles of θ near zero are poor (which corresponds to the formation of a singular matrix in the linear algebraic approach), it is not clear that the maximum θ corresponds to the optimum double spike. It seems more natural to us to directly consider the errors rather than focus on intermediate geometrical quantities such as θ. Geometrical quantities have a further disadvantage, in that they can be coordinate dependent: different values of θ arise from different choices of denominator isotope. The transformation from one isotope denominator to another does not preserve θ (transformations between isotope ratio spaces with different denominators are often approximately linear, but they are not orthogonal), and so results can depend on which denominator is used. The physical processes of mixing and mass fractionation are coordinate independent, and thus any scheme for choosing optimal double spikes should also be coordinate independent (Mel'nikov, 2005).

Both Galer (1999) and Johnson and Beard (1999) also consider linear error propagation, but both find results which again depend on which isotope is used in the denominator e.g. it is argued that lower errors are found in ^{206}Pb denominatored space than in ^{204}Pb denominatored space (Galer, 1999), and lower errors in ^{57}Fe denominatored space than in ^{54}Fe denominatored space (Johnson and Beard, 1999). However, error propagation should be no better or worse in one isotopic ratio space than another (Mel'nikov, 2005). The reason for coordinate dependent results by both these authors is likely the same: the assumption of uncorrelated isotopic ratios when performing linear error propagation (neglecting the off-diagonal terms in the covariance matrix). Uncorrelated isotopic ratios in one isotopic ratio space will be correlated in another isotopic ratio space. Assuming uncorrelated isotopic ratios in each isotopic ratio space leads to different answers for different isotopic ratio spaces. In our opinion, it is more appropriate to assume an error model based on independent ion beams (Dodson, 1969) than on a set of fixed errors on independent isotopic ratios. However, this criticism aside, methods that assume independent isotopic ratios still produce reasonable estimates of optimal double spikes with only slightly different results with different denominators.

The problem of assuming fixed errors on independent isotopic ratios affects a number of other studies, including those using Monte Carlo simulations (Fantle and Bullen, 2009). The approach of Fantle and Bullen (2009) also differs to that taken here in where errors are assumed to occur: Fantle and Bullen (2009) place errors on the standard and double spike composition and propagate these errors through the inversion, whereas we assume errors only on the mass spectrometer measurements. Propagating errors on the standard and double spike compositions essentially provides information about the accuracy of the technique i.e. the potential systematic bias, as the true standard and double spike compositions do not fluctuate. However, mass spectrometer measurements fluctuate, and propagating the measurement errors provides information on the precision of the technique. Both of these errors can be studied with the software we provide, but by default it is the precision we focus on. We agree with Fantle and Bullen (2009) that the error in Ca is minimised "using a [^{42}Ca*–^{48}Ca*] double spike composed of anywhere from 10 to 90% of the ^{42}Ca* ORNL single spike" (Fig. 5), but find that the optimum has slightly less double spike in the double spike-sample mix (more like 5% to 40% double spike rather than 25% to 55%).

An intriguing suggestion made by Galer (1999) is that of a "triple spike", a combination of three single spikes rather than two. Indeed, one can consider optimising for an arbitrary tracer composition rather than just a mixture of two particular single spikes. To do this is a little more demanding as the optimisation problem becomes higher dimensional, and multiple minima occur in the objective function. However, in our searching we have not found a scenario where a pure triple spike has a lower error than a pure double spike (and nor could Mel'nikov, 2005), but we cannot yet rule out such a possibility. The particular Pb triple spike suggested by Galer (1999) does produce low errors, but there are still double spikes with slightly lower error.

7. Conclusions

The main outcome of this work is the "double spike toolbox" software found in the electronic appendix. The software should make picking a good double spike easier for all experimenters. The optimal double spikes are decided purely on the basis of minimising error, and the software makes it easy to produce plots of error curves and surfaces to assess robustness to varying mixing proportions. While we have focused in this manuscript on the examples of Fe, Pb, and Ca, the software is completely general. In addition to the software, the "cocktail lists" provide a useful reference for quickly obtaining good double spike compositions. The source code to the software is freely available, and thus can be readily modified to satisfy the needs of individual users.

Acknowledgements

We are very grateful to R. L. Cline at Oak Ridge National Labs for providing us with the complete list of ORNL spike compositions. We thank Derek Vance and an anonymous reviewer for their constructive reviews, and thank David Rickard for his editorial handling. We also thank Ed Tipper, Andreas Stracke, and all the double spikers at IGMR ETH Zürich for helpful discussions and comments. The latest version of the software accompanying this manuscript can be found at www.johnrudge.com/doublespike.

Appendix A

A.1. The double spike inversion

The double spike inversion is based on the relative amounts of four isotopes, which can be conveniently expressed in terms of vectors of three isotopic ratios with a common denominator e.g. (^{56}Fe/^{54}Fe, ^{57}Fe/^{54}Fe, ^{58}Fe/^{54}Fe). Generally, it does not matter which isotope of the four is chosen as the common denominator: all choices will produce the same answer. The only exception to this is when one of the compositions contains none or almost none of a certain isotope, in which case that isotope should not be chosen as the denominator to avoid the numerical problems of dividing by very small quantities.

The key variables in the double spike inversion are shown in Fig. 1. The inversion is based on the following simple equations,

$$n_i = N_i e^{\alpha P_i}, \tag{6}$$

$$m_i = M_i e^{\beta P_i}, \tag{7}$$

$$M_i = \lambda T_i + (1-\lambda) N_i. \tag{8}$$

N_i refers to the ith isotopic ratio of the sample ($i=1, 2, 3$), e.g. $N_1 = (^{56}\mathrm{Fe}/^{54}\mathrm{Fe})_{\mathrm{sample}}$. M_i, m_i, and T_i are defined similarly (see Fig. 1).

P_i is the natural log of the ratio of the atomic masses e.g. $P_1 = \log(55.9349/53.9396)$. Eqs. (6) and (7) are exponential mass fractionation laws for the sample and the double spike-sample mixture, with mass fractionation factors α and β. Eq. (8) is the mixing relationship in isotope ratio space between double spike and sample (which is linear in the isotopic ratios as they have a common denominator). λ is related to the proportion p by mole in which the double spike and sample mix (Eq. (4)),

$$p = \left(1 + \frac{1-\lambda}{\lambda}\left(\frac{1 + \sum_k N_k}{1 + \sum_k T_k}\right)\right)^{-1}, \tag{9}$$

where Σ_k represents the sum over all isotope ratios for the element, not just the three ratios used in the inversion. Note that λ depends on which isotope is used as a denominator, unlike α and β which are coordinate independent.

Eqs. (6), (7), and (8) can be combined to give

$$F_i(\lambda, \alpha, \beta, \mathbf{n}, \mathbf{m}, \mathbf{T}) = \lambda T_i + (1-\lambda) n_i e^{-\alpha P_i} - m_i e^{-\beta P_i} = 0, \tag{10}$$

where $\mathbf{n} = (n_1, n_2, n_3)$ etc. This is a set of three non-linear equations, which can be solved to find the three unknowns λ, α, and β.

If α and β are small ($\alpha, \beta \ll 1$), these equations can be linearised,

$$F_i(\lambda, \alpha, \beta, \mathbf{n}, \mathbf{m}, \mathbf{T}) \approx n_i - m_i + \lambda(T_i - n_i) - (1-\lambda)\alpha n_i P_i + \beta m_i P_i, \tag{11}$$

and written in matrix form as

$$\mathbf{F}(\mathbf{x}, \mathbf{n}, \mathbf{m}, \mathbf{T}) \approx -\mathbf{b} + A\mathbf{x}, \tag{12}$$

where

$$A = \begin{pmatrix} T_1 - n_1 & -n_1 P_1 & m_1 P_1 \\ T_2 - n_2 & -n_2 P_2 & m_2 P_2 \\ T_3 - n_3 & -n_3 P_3 & m_3 P_3 \end{pmatrix}, \quad \mathbf{b} = \begin{pmatrix} m_1 - n_1 \\ m_2 - n_2 \\ m_3 - n_3 \end{pmatrix}, \quad \mathbf{x} = \begin{pmatrix} \lambda \\ (1-\lambda)\alpha \\ \beta \end{pmatrix}. \tag{13}$$

Thus for small fractionations, the double spike inversion is simply a matter of solving the linear equations $A\mathbf{x} = \mathbf{b}$ for $\mathbf{x}$, and then obtaining λ, α, and β from $\mathbf{x}$ (Dodson, 1970; Dallwitz, 1970).

For larger α and β, we must solve the full non-linear equations

$$\mathbf{F}(\mathbf{x}, \mathbf{n}, \mathbf{m}, \mathbf{T}) = 0. \tag{14}$$

This can be done effectively by iterative methods (e.g. Newton–Raphson) (Albarède and Beard, 2004). A good starting point for the iteration is provided by the linear solution, and the following analytical Jacobian can be used to aid the iteration

$$\frac{\partial \mathbf{F}}{\partial \mathbf{x}} = \begin{pmatrix} T_1 - n_1 e^{-\alpha P_1}(1 + \alpha P_1) & -n_1 P_1 e^{-\alpha P_1} & m_1 P_1 e^{-\beta P_1} \\ T_2 - n_2 e^{-\alpha P_2}(1 + \alpha P_2) & -n_2 P_2 e^{-\alpha P_2} & m_2 P_2 e^{-\beta P_2} \\ T_3 - n_3 e^{-\alpha P_3}(1 + \alpha P_3) & -n_3 P_3 e^{-\alpha P_3} & m_3 P_3 e^{-\beta P_3} \end{pmatrix}. \tag{15}$$

The iteration is performed in the software using fsolve, MATLAB's non-linear equation solving routine. An alternative geometrically motivated way of performing the iteration can be found in Siebert et al. (2001).

Appendix B. Error propagation

Standard linear error propagation can be used to calculate the errors in $\mathbf{x}$ given the errors in $\mathbf{n}$, $\mathbf{m}$, and $\mathbf{T}$ (Hamelin et al., 1985). Let $V_\mathbf{x}$, $V_\mathbf{n}$, $V_\mathbf{m}$ and $V_\mathbf{T}$ be the corresponding covariance matrices. Assuming the errors in $\mathbf{n}$, $\mathbf{m}$ and $\mathbf{T}$ are independent of one another, the covariance matrix $V_\mathbf{x}$ is given by

$$V_\mathbf{x} = \frac{\partial \mathbf{x}}{\partial \mathbf{n}} \cdot V_\mathbf{n} \cdot \frac{\partial \mathbf{x}^T}{\partial \mathbf{n}} + \frac{\partial \mathbf{x}}{\partial \mathbf{m}} \cdot V_\mathbf{m} \cdot \frac{\partial \mathbf{x}^T}{\partial \mathbf{m}} + \frac{\partial \mathbf{x}}{\partial \mathbf{T}} \cdot V_\mathbf{T} \cdot \frac{\partial \mathbf{x}^T}{\partial \mathbf{T}}, \tag{16}$$

where

$$\frac{\partial \mathbf{x}}{\partial \mathbf{n}} = -\left(\frac{\partial \mathbf{F}}{\partial \mathbf{x}}\right)^{-1} \frac{\partial \mathbf{F}}{\partial \mathbf{n}}, \tag{17}$$

$$\frac{\partial \mathbf{x}}{\partial \mathbf{m}} = -\left(\frac{\partial \mathbf{F}}{\partial \mathbf{x}}\right)^{-1} \frac{\partial \mathbf{F}}{\partial \mathbf{m}}, \tag{18}$$

$$\frac{\partial \mathbf{x}}{\partial \mathbf{T}} = -\left(\frac{\partial \mathbf{F}}{\partial \mathbf{x}}\right)^{-1} \frac{\partial \mathbf{F}}{\partial \mathbf{T}}, \tag{19}$$

and

$$\frac{\partial F_i}{\partial n_j} = (1-\lambda) e^{-\alpha P_i} \delta_{ij}, \quad \frac{\partial F_i}{\partial m_j} = -e^{-\beta P_i} \delta_{ij}, \quad \frac{\partial F_i}{\partial T_j} = \lambda \delta_{ij}, \tag{20}$$

where δ_{ij} is the Kronecker delta. The covariance matrix for $\mathbf{y} = (\lambda, \alpha, \beta)^T$ can be calculated from the covariance matrix of $\mathbf{x} = (\lambda, (1-\lambda)\alpha, \beta)^T$ by

$$V_\mathbf{y} = \frac{\partial \mathbf{y}}{\partial \mathbf{x}} \cdot V_\mathbf{x} \cdot \frac{\partial \mathbf{y}^T}{\partial \mathbf{x}}, \tag{21}$$

where

$$\frac{\partial \mathbf{y}}{\partial \mathbf{x}} = \begin{pmatrix} 1 & 0 & 0 \\ \alpha/(1-\lambda) & 1/(1-\lambda) & 0 \\ 0 & 0 & 1 \end{pmatrix}. \tag{22}$$

The error propagation for $\mathbf{N}$ can be done in a similar fashion,

$$V_\mathbf{N} = \frac{\partial \mathbf{N}}{\partial \mathbf{n}} \cdot V_\mathbf{n} \cdot \frac{\partial \mathbf{N}^T}{\partial \mathbf{n}} + \frac{\partial \mathbf{N}}{\partial \mathbf{m}} \cdot V_\mathbf{m} \cdot \frac{\partial \mathbf{N}^T}{\partial \mathbf{m}} + \frac{\partial \mathbf{N}}{\partial \mathbf{T}} \cdot V_\mathbf{T} \cdot \frac{\partial \mathbf{N}^T}{\partial \mathbf{T}}, \tag{23}$$

where the partial derivatives of $\mathbf{N}$ can be calculated from Eq. (6) as

$$\frac{\partial N_i}{\partial n_j} = \delta_{ij} e^{-\alpha P_i} - P_i n_i e^{-\alpha P_i} \frac{\partial \alpha}{\partial n_j}, \tag{24}$$

$$\frac{\partial N_i}{\partial m_j} = -P_i n_i e^{-\alpha P_i} \frac{\partial \alpha}{\partial m_j}, \tag{25}$$

$$\frac{\partial N_i}{\partial T_j} = -P_i n_i e^{-\alpha P_i} \frac{\partial \alpha}{\partial T_j}. \tag{26}$$

The partial derivatives of α in the above can be found from the second rows of $\partial\mathbf{y}/\partial\mathbf{n}$, $\partial\mathbf{y}/\partial\mathbf{m}$ and $\partial\mathbf{y}/\partial\mathbf{T}$, given by Eqs. (17), (18), (19), and (22) as

$$\frac{\partial \mathbf{y}}{\partial \mathbf{n}} = \frac{\partial \mathbf{y}}{\partial \mathbf{x}} \cdot \frac{\partial \mathbf{x}}{\partial \mathbf{n}}, \tag{27}$$

$$\frac{\partial \mathbf{y}}{\partial \mathbf{m}} = \frac{\partial \mathbf{y}}{\partial \mathbf{x}} \cdot \frac{\partial \mathbf{x}}{\partial \mathbf{m}}, \tag{28}$$

$$\frac{\partial \mathbf{y}}{\partial \mathbf{T}} = \frac{\partial \mathbf{y}}{\partial \mathbf{x}} \cdot \frac{\partial \mathbf{x}}{\partial \mathbf{T}}. \tag{29}$$

Finally, the covariance matrix $V_\mathbf{M}$ is given by

$$V_\mathbf{M} = \frac{\partial \mathbf{M}}{\partial \mathbf{n}} \cdot V_\mathbf{n} \cdot \frac{\partial \mathbf{M}^T}{\partial \mathbf{n}} + \frac{\partial \mathbf{M}}{\partial \mathbf{m}} \cdot V_\mathbf{m} \cdot \frac{\partial \mathbf{M}^T}{\partial \mathbf{m}} + \frac{\partial \mathbf{M}}{\partial \mathbf{T}} \cdot V_\mathbf{T} \cdot \frac{\partial \mathbf{M}^T}{\partial \mathbf{T}}, \tag{30}$$

where the partial derivatives of $\mathbf{M}$ can be calculated from Eq. (7) as

$$\frac{\partial M_i}{\partial n_j} = -P_i m_i e^{-\beta P_i} \frac{\partial \beta}{\partial n_j}, \tag{31}$$

$$\frac{\partial M_i}{\partial m_j} = \delta_{ij} e^{-\beta P_i} - P_i m_i e^{-\beta P_i} \frac{\partial \beta}{\partial m_j}, \tag{32}$$

$$\frac{\partial M_i}{\partial T_j} = -P_i m_i e^{-\beta P_i} \frac{\partial \beta}{\partial T_j}, \tag{33}$$

and the partial derivatives of β can be found from the third rows of $\partial\mathbf{y}/\partial\mathbf{n}$, $\partial\mathbf{y}/\partial\mathbf{m}$ and $\partial\mathbf{y}/\partial\mathbf{T}$.

Appendix C. Error model

Consider n ion beams with intensities in volts given by the random variables $I_1, I_2, \ldots, I_n$. We will assume that each beam intensity is independent and normally distributed, with means μ_j and variances

$$\sigma_j^2 = a_j + b_j\mu_j + c_j\mu_j^2, \tag{34}$$

for some specified error parameters a_j, b_j, and c_j (Dodson, 1969). The relative values of the means μ_j are determined by the isotopic composition of the substance being measured. We will assume the mean total intensity $\Sigma_j\mu_j$ is set at some fixed value (10 V by default, but this can be adjusted in the software). For the variances, we use a simple model of an ion beam that incorporates Johnson–Nyquist noise in the amplifiers (for a_j) and counting statistics (for b_j):

$$a_j = \frac{4kTR}{\Delta t}, \quad b_j = \frac{eR}{\Delta t}, \quad c_j = 0, \tag{35}$$

where k is the Boltzmann constant 1.3806504×10^{-23} J K^{-1} and e is the elementary charge $1.602176487\times10^{-19}$ C. The remaining constants are properties of the mass spectrometer, which we have chosen defaults as follows: the resistance $R=10^{11}$ Ω, the temperature $T=300$ K, and the integration time $\Delta t=8$ s.

The beam covariance matrix is diagonal,

$$V_{\mathbf{I}} = \begin{pmatrix} \sigma_1^2 & 0 & \cdots & 0 \\ 0 & \sigma_2^2 & \cdots & 0 \\ 0 & 0 & \ddots & \vdots \\ 0 & 0 & \cdots & \sigma_n^2 \end{pmatrix}. \tag{36}$$

In order to perform the error propagation of the previous section, the covariance matrix of the ratios is needed. Suppose we use the last isotope as the denominator, taking ratios $R_1=I_1/I_n$, $R_2=I_2/I_n,\ldots$, $R_{n-1}=I_{n-1}/I_n$. Then the covariance matrix of the ratios is

$$V_{\mathbf{R}} = \frac{\partial \mathbf{R}}{\partial \mathbf{I}} \cdot V_{\mathbf{I}} \cdot \frac{\partial \mathbf{R}^T}{\partial \mathbf{I}}, \tag{37}$$

where

$$\frac{\partial \mathbf{R}}{\partial \mathbf{I}} = \begin{pmatrix} 1/I_n & 0 & \cdots & 0 & -I_1/I_n^2 \\ 0 & 1/I_n & \cdots & 0 & -I_2/I_n^2 \\ \vdots & & \ddots & \vdots & \vdots \\ 0 & 0 & \cdots & 1/I_n & -I_{n-1}/I_n^2 \end{pmatrix}. \tag{38}$$

Note that the covariance matrix of the ratios is certainly not diagonal. The software uses the above error model by default, but can be customised if needed e.g. it is possible to manually adjust the error parameters a_j, b_j, and c_j, which can be used to incorporate some types of additional error.

An important source of additional error that can affect the internal precision arises from the corrections that are made to account for interferences. For example, corrections are often made for interfering isotopes of the same mass (isobaric interferences) e.g. the interference of ^{58}Ni during measurement of ^{58}Fe. This interference is usually corrected for by measuring neighbouring masses (in this case, ^{60}Ni) and applying an approximate correction factor based on an assumed ^{58}Ni/^{60}Ni ratio and an assumed mass fractionation. The additional noise this correction induces on the ^{58}Fe measurement depends on the strength of the ^{60}Ni ion beam, and taking this into account requires a more sophisticated error model than that described above. However, an approximate treatment is to simply increase the value of a_j corresponding to the ^{58}Fe beam by an appropriate amount. For example, a typical correction formula is

$$I_{58c} = I_{58} - \left(\frac{^{58}\mathrm{Ni}}{^{58}\mathrm{Ni}}\right)_{\mathrm{std}} \left(\frac{57.9353}{59.9308}\right)^{\beta_{\mathrm{Ni}}} I_{60}, \tag{39}$$

where I_{58} and I_{60} are the measured beam intensities at masses 58 and 60, and I_{58c} is the mass 58 beam intensity corrected for Ni interference. 57.9353 and 59.9308 are the atomic masses of ^{58}Ni and ^{60}Ni respectively. With an assumed standard value $(^{58}\mathrm{Ni}/^{60}\mathrm{Ni})_{\mathrm{std}}=2.596$ and assumed mass bias $\beta_{\mathrm{Ni}}=1.6$, the correction is

$$I_{58c} = I_{58} - 2.459 I_{60}, \tag{40}$$

and thus the noise on the corrected intensity is

$$\sigma_{58c}^2 = \sigma_{58}^2 + 6.047\sigma_{60}^2. \tag{41}$$

Typically, the magnitude of the mass 60 beam is quite small, and so its error is dominated by thermal noise rather than counting statistics, i.e.

$$\sigma_{60}^2 \approx \frac{4kTR}{\Delta t}. \tag{42}$$

Thus an approximate method for modelling the noise due to the interference correction is to change the coefficient a_j on the 58 mass to

$$a_{58} = 7.047 \times \frac{4kTR}{\Delta t}. \tag{43}$$

A commonly encountered issue in MC-ICP-MS work is the effect of the acid "blank" that is used to dissolve the sample. The blank can form a large part of the baseline, but can be corrected for by measuring an "on-peak zero", a measurement of the acid excluding the sample (Nelms, 2005). By subtracting the on-peak zero measurement from the measurement of the spike-sample mixture, an additional source of noise is introduced due to the additional measurement. This can similarly be included in the error model by increasing the coefficients a_j appropriately.

There are many other kinds of interferences that occur in different situations, and each must be dealt with on a case by case basis. It should be noted that not all interferences can be corrected for, and that some of the corrections applied are only approximate e.g. the correction formula in Eq. (39) is only approximate as the standard value and mass bias take assumed values and not actual values. Uncorrected interferences can lead to serious biases and inaccuracies in any isotopic measurements and must be avoided where possible.

Appendix D. Optimal double spikes

The most natural criterion for a good double spike is one which minimises the error on a quantity of interest. However, different quantities are of interest in different situations. For stable isotope work, the

most natural quantity to focus on is α, the fractionation factor which describes the mass fractionation between the sample **N** and the standard composition **n**. The error on α can be obtained from the middle element of the matrix $V_{\mathbf{y}}$ in Eq. (21). However, for radiogenic isotope work, where the composition **n** is a measured quantity (the unspiked run), it is not clear that α is the appropriate quantity of interest. Instead, a more natural quantity to minimise could be the error on a particular ratio, i.e. N_j for some choice of j, which can be obtained from the diagonal entries of the matrix $V_{\mathbf{N}}$ in Eq. (23). The different choices of error to minimise will lead to different optimal double spikes.

A double spike consists of a mixture of two single spikes which may or may not have impurities. We mix a proportion q (by mole of element) of the first spike to $1-q$ of the second spike to make the double spike (Fig. 1). The double spike is added to the sample in proportion p of spike to $1-p$ of sample. Finding the optimal double spike is simply a matter of finding the values of the proportions p and q that minimise the appropriate error. This is a 2D optimisation problem that can be solved quickly and efficiently by gradient based methods. As can be seen in Fig. 2, the objective function appears to be convex with a single minimum (it is bowl-shaped), which makes optimisation particularly straightforward. It should be noted that error estimates also depend on α and β (and hence the sample composition). By default α and β are set to zero in the software during optimisation. However, the error estimates vary very little for reasonable values of α and β (between -2 and 2), and thus this dependence on α and β can be neglected.

Appendix E. δ and parts per million notation

For stable isotope work, the main quantity of interest is α, the natural mass fractionation factor. However, α is not usually quoted in the experimental results. Instead, results are usually presented in terms of the isotopic ratios, either as δ values, as parts per million (ppm), or as part per million per atomic mass unit (ppm per amu). These are defined by

$$\delta^i = 10^3\left(\frac{N_i}{n_i}-1\right), \tag{44}$$

$$\mathrm{ppm}^i = 10^6\left(\frac{N_i}{n_i}-1\right), \tag{45}$$

$$\mathrm{ppm\,per\,amu}^i = \frac{10^6}{\Delta_i A}\left(\frac{N_i}{n_i}-1\right), \tag{46}$$

where $\Delta_i A$ is the difference in atomic masses between the two isotopes e.g. $\Delta_1 A = 55.9349 - 53.9396$. The ratios N_i/n_i (sample over standard) are related to α through the exponential mass fractionation law (6),

$$-\alpha P_i = \log\frac{N_i}{n_i}. \tag{47}$$

The above equation has prompted some authors to report their results using the logarithm of the ratios (Hulston and Thode, 1965; Young et al., 2002), which is much more convenient when comparing with α,

$$\delta'^i = 10^3 \log\frac{N_i}{n_i} = -10^3\alpha P_i, \tag{48}$$

$$\mathrm{ppm}'^i = 10^6 \log\frac{N_i}{n_i} = -10^6\alpha P_i, \tag{49}$$

$$\mathrm{ppm\,per\,amu}'^i = \frac{10^6}{\Delta_i A}\log\frac{N_i}{n_i} = -10^6\frac{\alpha P_i}{\Delta_i A}. \tag{50}$$

These quantities are simple linear rescalings of α, and thus minimising the error on α is equivalent to minimising the error on any of these quantities. In most practical cases, the logarithmic quantities (Eqs. (48)–(50)) differ a little from the original quantities (Eqs. (44)–(46)), as they are related by linear approximation about $N_i/n_i = 1$. Also, since the differences in atomic masses of the isotopes are usually small compared to the atomic masses themselves, we can make an approximation to Eq. (50) as

$$\mathrm{ppm\,per\,amu}' \approx -10^6\frac{\alpha}{\overline{A}} \tag{51}$$

where $\overline{A}$ is a mean or typical atomic mass for the element under consideration. The above rescaling is used in Tables 1, 2, and 4.

Appendix F. Calibration

F.1. Standard calibration

It is vital for the accuracy of the double spike technique that the double spike and standard be well calibrated. For standard calibration, it is only important to know the mass fractionation line the standard lies on, rather than the absolute composition of the standard, since all results are generally quoted relative to the standard value. This can be clearly seen from the governing equations. The double spike equations (Eq. (10)) are

$$\lambda T_i + (1-\lambda)n_i e^{-\alpha P_i} - m_i e^{-\beta P_i} = 0. \tag{52}$$

Suppose instead of the true standard composition **n**, we use an alternate standard composition $\mathbf{n}'$ in the inversion, which lies at a different point along the mass fractionation line, given by a mass fractionation factor α_0,

$$n'_i = n_i e^{\alpha_0 P_i}. \tag{53}$$

Multiplying Eq. (52) by $e^{\alpha_0 P_i}$, we have

$$\lambda T_i e^{\alpha_0 P_i} + (1-\lambda)n_i e^{(\alpha_0-\alpha)P_i} - m_i e^{(\alpha_0-\beta)P_i} = 0, \tag{54}$$

which can be rewritten in exactly the same form as Eq. (52),

$$\lambda' T'_i + (1-\lambda')n'_i e^{-\alpha' P_i} - m_i e^{-\beta' P_i} = 0, \tag{55}$$

where

$$T'_i = T_i e^{\alpha_0 P_i}, \tag{56}$$

$$\lambda' = \lambda, \tag{57}$$

$$\alpha' = \alpha, \tag{58}$$

$$\beta' = \beta - \alpha_0. \tag{59}$$

Thus provided the double spike $\mathbf{T}'$ is calibrated relative to the alternate standard value $\mathbf{n}'$, the only difference in the inversion will be in the values of β. α is unchanged, and thus the composition of the sample relative to the standard can be determined even if the absolute composition of the standard is not known.

F.2. Double spike calibration

One way of performing the double spike calibration is by measuring a series of double spike-standard mixtures in different proportions (Dodson, 1963). Suppose J different double spike-standard mixtures

are measured as the set of isotopic ratios m_i^j; $i=1,2,3$; $j=1,\ldots,J$. These measurements satisfy the double spike equations (Eq. (10))

$$\lambda^j T_i + \left(1-\lambda^j\right) n_i - m_i^j e^{-\beta^j P_i} = 0, \tag{60}$$

where λ^j are the J mixing proportions and β^j are the J instrumental fractionation factors. Note that α does not appear in the above expression because it is the standard itself that is used in the mixtures. It is convenient to rewrite the double spike composition **T** in terms of its difference from the standard value **n** (assumed known),

$$T_i = n_i + \zeta u_i, \tag{61}$$

where **u** is a unit vector along the double spike-sample mixing line, and ζ is a scalar. Eq. (60) can be rewritten as

$$n_i + \zeta\lambda^j u_i - m_i^j e^{-\beta^j P_i} = 0. \tag{62}$$

Letting $\mu^j=\zeta\lambda^j$, this becomes

$$n_i + \mu^j u_i - m_i^j e^{-\beta^j P_i} = 0. \tag{63}$$

This a set of $3J$ equations in $2J+2$ unknowns: the J unknown values of β^j, the J unknown values of μ^j, and the 2 unknown independent components of the unit vector **u** (e.g. as specified by two angles θ and ϕ in spherical co-ordinates). At least two different mixing proportions ($J=2$) are required to solve these equations. If further mixtures are measured ($J>2$) then the above system of equations is overdetermined and can be solved in a least squares sense, potentially improving the precision of the double spike calibration.

While solution of the equations above determines the double spike-sample mixing line (the unit vector **u** can be calculated), the position of the double spike along this line is not determined: There is a trade off between ζ and the a^j, as only their product $\mu^j=\zeta\lambda^j$ can be determined. There are two main ways to determine the actual position of the double spike along the double spike-sample mixing line. One way is to use very careful weighing to determine the mixing proportions accurately. The other way is to use a second standard material (ideally with a composition quite different to the first standard) and perform another series of standard-double spike mixtures with this second standard. The intersection of the two standard-double spike mixing lines should then provide an accurate calibration of the double spike composition.

It is possible estimate to the bias that arises from using a double spike composition which lies at the wrong point along the double spike-standard mixing line. For example, suppose that instead of using the true double spike composition **T** in the inversion, we use a different double spike composition **T**′ that lies at a different point along the double spike-standard mixing line, namely

$$T_i' = \rho T_i + (1-\rho) n_i, \tag{64}$$

for some ρ. If $\rho=1$, the double spike has been calibrated perfectly, otherwise there is a bias. If we look at the corresponding linear equations (Eq. (13)) for the miscalibrated double spike **T**′ we have

$$A' = \begin{pmatrix} \rho(T_1-n_1) & -n_1P_1 & m_1P_1 \\ \rho(T_2-n_2) & -n_2P_2 & m_2P_2 \\ \rho(T_3-n_3) & -n_3P_3 & m_3P_3 \end{pmatrix}, \tag{65}$$

$$\mathbf{b}' = \begin{pmatrix} m_1-n_1 \\ m_2-n_2 \\ m_3-n_3 \end{pmatrix}, \quad \mathbf{x}' = \begin{pmatrix} \lambda' \\ (1-\lambda')\alpha' \\ \beta' \end{pmatrix}.$$

Thus the linear inversion solutions with the true double spike **T** and the miscalibrated double spike **T**′ are related through

$$\frac{\lambda'}{\lambda} - 1 = \frac{1-\rho}{\rho}, \tag{66}$$

$$\frac{\alpha'}{\alpha} - 1 = \frac{\lambda(1-\rho)}{\rho-\lambda}, \tag{67}$$

$$\frac{\beta'}{\beta} - 1 = 0. \tag{68}$$

The above can also be expressed using proportion by mole of element instead of in ratio space as

$$\frac{p'}{p} - 1 = \frac{1-r}{r}, \tag{69}$$

$$\frac{\alpha'}{\alpha} - 1 = \frac{p(1-r)}{r-p}, \tag{70}$$

$$\frac{\beta'}{\beta} - 1 = 0, \tag{71}$$

where p is the proportion per mole of double spike in the double spike-sample mix (related to λ by Eq. (9)), and r is the proportion per mole of true double spike in the miscalibrated double spike (related to ρ). As an example, suppose the miscalibrated double spike had $r=0.99$ (i.e. has a composition per mole of 99% of the true double spike value, with a contamination of 1% of the standard), and that the double spike-sample mixing proportion $p=0.5$, then the resulting bias in α from Eq. (70) is 0.0102 (i.e. a 1.02% relative bias). The potential biases for the full non-linear inversion can be explored in more detail using the software, but the above equations give a good approximation.

Appendix G. Experimental details

The Fe isotope analyses were carried out on the Nu Plasma 1700 high-resolution MC-ICP-MS (at ETH Zürich) in normal dry plasma mode. The Nu Plasma 1700 provides true mass-resolution (defined by the peak width, $m/\Delta m$) from an adjustable source defining slit and individual adjustable collector slit widths, which allow the complete resolution of the polyatomic isobaric interferences, including ArO^+, ArN^+, and CaO^+. The four Fe ion beams were collected simultaneously on Faraday collectors, equipment with 10^{11} Ω resistors, but with a dynamic range of 20 V. The direct interferences of $^{54}Cr^+$ and $^{58}Ni^+$ were assessed and corrected for by the simultaneous measurement of ^{52}Cr, ^{53}Cr, ^{60}Ni, and ^{61}Ni. The ~200 ppb Fe solutions in 0.1 M HCl were introduced into the plasma via an Aridus II desolvator equipped with a PFA nebuliser and using a 60–80 µl/min uptake rate. Analyses consisted of 100×4 s integrations and a 5 minute wash cycle between spiked standards. Background levels are reduced to $<10^{-13}$ A for $^{56}Fe^+$ between measurements.

Appendix H. Supplementary data

Supplementary data associated with this article can be found, in the online version, at doi:10.1016/j.chemgeo.2009.05.010.

References

Albarède, F., Beard, B., 2004. Analytical methods for non-traditional isotopes. Rev. Mineral. Geochem. 55, 113–152. doi:10.2138/gsrmg.55.1.113.

Albarède, F., Telouk, P., Blichert-Toft, J., Boyet, M., Agranier, A., Nelson, B., 2004. Precise and accurate isotopic measurements using multiple-collector ICPMS. Geochim. Cosmochim. Acta 12, 2725–2744. doi:10.1016/j.gca.2003.11.024.

Compston, W., Oversby, V.M., 1969. Lead isotopic analysis using a double spike. J. Geophys. Res. 74, 4338–4348.

Cumming, G.L., 1973. Propagation of experimental errors in lead isotope ratio measurements using the double spike method. Chem. Geol. 11, 157–165. doi:10.1016/0009-2541(73) 90014-4.
Dallwitz, M.J., 1970. Fractionation corrections in lead isotopic analysis. Chem. Geol. 6, 311–314. doi:10.1016/0009-2541(70)90032-X.
DePaolo, D.J., 2004. Calcium isotopic variations produced by biological, kinetic, radiogenic and nucleosynthetic processes. Rev. Mineral. Geochem. 55, 255–288. doi:10.2138/gsrmg.55.1.255.
Dodson, M.H., 1963. A theoretical study of the use of internal standards for precise isotopic analysis by the surface ionization technique: part I — general first-order algebraic solutions. J. Sci. Instrum. 40, 289–295. doi:10.1088/0950-7671/40/6/307.
Dodson, M.H., 1969. A theoretical study of the use of internal standards for precise isotopic analysis by the surface ionization technique part II: error relationships. J. Phys. E: Sci. Instrum. 2, 490–498. doi:10.1088/0022-3735/2/6/306.
Dodson, M.H., 1970. Simplified equations for double-spiked isotopic analyses. Geochim. Cosmochim. Acta 34, 1241–1244. doi:10.1016/0016-7037(70)90060-8.
Fantle, M.S., Bullen, T.D., 2009. Essentials of iron, chromium, and calcium isotope analysis of natural materials by thermal ionization mass spectrometry. Chem. Geol. 258, 50–64. doi:10.1016/j.chemgeo.2008.06.018.
Feineman, M., Penniston-Dorland, S., Poitrasson, F., Weyer, S., 2009. Applications of non-traditional stable isotopes in high-temperature geochemistry. Chem. Geol. 258, 1–4. doi:10.1016/j.chemgeo.2008.08.008.
Galer, S.J.G., 1999. Optimal double and triple spiking for high precision lead isotopic measurement. Chem. Geol. 157, 255–274. doi:10.1016/S0009-2541(98)00203-4.
Galer, S.J.G., 2007. The double-spike cookbook. 17th Annual V. M. Goldschmidt Conference Cologne. doi:10.1016/j.gca.2007.06.016.
Galer, S.J.G., 2008. A smorgasbord of double spikes for the discerning gourmet. AGU Fall Meeting.
Gopalan, K., Macdougall, D., Macisaac, C., 2006. Evaluation of a ^{42}Ca–^{43}Ca double-spike for high precision Ca isotope analysis. Int. J. Mass Spectrom. 248, 9–16. doi:10.1016/j.ijms.2005.09.009.
Gopalan, K., Macdougall, J.D., Macisaac, C., 2007. High precision determination of ^{48}Ca/^{42}Ca ratio by TIMS for Ca isotope fractionation studies. Geostand. Geoanal. Res. 31, 227–236. doi:10.1111/j.1751-908X.2007.00847.x.
Hamelin, B., Manhesa, G., Albarède, F., Allègre, C.J., 1985. Precise lead isotope measurements by the double spike technique: a reconsideration. Geochim. Cosmochim. Acta 49, 173–182. doi:10.1016/0016-7037(85)90202-9.
Hofmann, A., 1971. Fractionation corrections for mixed-isotope spikes of Sr, K, and Pb. Earth Planet. Sci. Lett. 10, 397–402. doi:10.1016/0012-821X(71)90087-2.
Holmden, C., 2005. Measurement of δ^{44}Ca using ^{43}Ca–^{42}Ca a double-spike TIMS technique. Summary of Investigations, Sask. Industry Resources, Misc. Rep. 2005-1, vol. 1, pp. 1–7.
Hulston, J.R., Thode, H.G., 1965. Variations in the S^{33}, S^{34}, and S^{36} contents of meteorites and their relation to chemical and nuclear effects. J. Geophys. Res. 70, 3475–3484.
Johnson, C.M., Beard, B.L., 1999. Correction of instrumentally produced mass fractionation during isotopic analysis of Fe by thermal ionization mass spectrometry. Int. J. Mass Spectrom. 193, 87–99. doi:10.1016/S1387-3806(99)00158-X.
Kehm, K., Hauri, E.H., Alexander, C.M.O., Carlson, R.W., 2003. High precision iron isotope measurements of meteoritic material by cold plasma ICP-MS. Geochim. Cosmochim. Acta 67, 2879–2891. doi:10.1016/S0016-7037(03)00080-2.
Konter, J.G., Pietruszka, A.J., Hanan, B.B., 2008a. Development of a ^{58}Fe–^{57}Fe double spike for Fe isotopic analysis using a Nu Plasma 1700 MC-ICP-MS. 18th Annual V.M. Goldschmidt Conference Vancouver. doi:10.1016/j.gca.2008.05.014.
Konter, J.G., Pietruszka, A.J., Hanan, B.B., 2008b. Evaluation of double and triple spike Fe isotope measurements and results for basaltic lavas. AGU Fall meeting.
Lacan, F., Radic, A., Jeandel, C., Poitrasson, F., Sarthou, G., Pradoux, C., Freydier, R., 2008. Measurement of the isotopic composition of dissolved iron in the open ocean. Geophys. Res. Lett. 35, L24610. doi:10.1029/2008GL035841.
Mel'nikov, N., 2005. Errors of the double spiking technique in the isotopic analysis of common lead. Geochem. Int. 43, 1228–1234.
Nelms, S. (Ed.), 2005. Inductively Coupled Plasma Mass Spectrometry Handbook. Wiley-Blackwell.
Rosman, K.J.R., Taylor, P.D.P., 1998. Isotopic compositions of the elements 1997. J. Phys. Chem. Ref. Data 27, 1275–1288.
Russell, R.D., 1971. The systematics of double spiking. J. Geophys. Res. 76, 4949–4955.
Russell, W.A., Papanastassiou, D.A., 1978. Calcium isotope fractionation in ion-exchange chromatography. Anal. Chem. 50, 1151–1154. doi:10.1021/ac50030a036.
Russell, W.A., Papanastassiou, D.A., Tombrello, T.A., 1978. Ca isotope fractionation on the Earth and other solar system materials. Geochim. Cosmochim. Acta 42, 1075–1090. doi:10.1016/0016-7037(78)90105-9.
Siebert, C., Nägler, T.F., Kramers, J.D., 2001. Determination of molybdenum isotope fractionation by double-spike multicollector inductively coupled plasma mass spectrometry. Geochem. Geophys. Geosys. 2, 1032. doi:10.1029/2000GC000124.
Thirlwall, M., Anczkiewicz, R., 2004. Multidynamic isotope ratio analysis using MC-ICP-MS and the causes of secular drift in Hf, Nd and Pb isotope ratios. Int. J. Mass Spectrom. 235, 59–81. doi:10.1016/j.ijms.2004.04.002.
Thirlwall, M.F., 2002. Multicollector ICP-MS analysis of Pb isotopes using a ^{207}Pb–^{204}Pb double spike demonstrates up to 400 ppm/amu systematic errors in Tl-normalization. Chem. Geol. 184, 255–279. doi:10.1016/S0009-2541(01)00365-5.
Vance, D., Thirlwall, M.F., 2002. An assessment of mass discrimination in MC-ICPMS using Nd isotopes. Chem. Geol. 185, 227–240. doi:10.1016/S0009-2541(01)00402-8.
Young, E.D., Galy, A., Nagahara, H., 2002. Kinetic and equilibrium mass-dependent isotope fractionation laws in nature and their geochemical and cosmochemical significance. Geochim. Cosmochim. Acta 66, 1095–1104. doi:10.1016/S0016-7037(01)00832-8.